Atmospheric Environment 45 (2011) 387–394

Contents lists available at ScienceDirect

Atmospheric Environment

journal homepage: www.elsevier.com/locate/atmosenv

Radiative forcing due to changes in ozone and methane caused by the transport sector

G. Myhre [a,b,*], K.P. Shine [c], G. Rädel [c], M. Gauss [b,k], I.S.A. Isaksen [a,b], Q. Tang [d], M.J. Prather [d], J.E. Williams [e], P. van Velthoven [e], O. Dessens [f], B. Koffi [g], S. Szopa [g], P. Hoor [h], V. Grewe [i], J. Borken-Kleefeld [j,1], T.K. Berntsen [a,b], J.S. Fuglestvedt [a]

[a] Center for International Climate and Environmental Research-Oslo (CICERO), Oslo, Norway
[b] Department of Geosciences, University of Oslo, Norway
[c] Department of Meteorology, University of Reading, Reading, UK
[d] Earth System Science Dept., UC Irvine, CA, USA
[e] Chemistry-Climate Division, Royal Netherlands Meteorological Institute, The Netherlands
[f] Centre for Atmospheric Science, Dept. of Chemistry, Cambridge, UK
[g] Laboratoire des Sciences du Climat et de l'Environnement (LSCE-IPSL), Gif-sur-Yvette, France
[h] Institute for Atmospheric Physics, University Mainz, Germany
[i] Deutsches Zentrum für Luft- und Raumfahrt, Institut für Physik der Atmosphäre, Oberpfaffenhofen, Germany
[j] Formerly: Deutsches Zentrum für Luft- und Raumfahrt, Verkehrsstudien, Berlin, Germany
[k] Norwegian Meteorological Institute, Oslo, Norway

ARTICLE INFO

Article history:
Received 19 May 2010
Received in revised form
27 September 2010
Accepted 4 October 2010

Keywords:
Radiative forcing
GWP
GTP
Shipping
Aviation
Road transport

ABSTRACT

The year 2000 radiative forcing (RF) due to changes in O_3 and CH_4 (and the CH_4-induced stratospheric water vapour) as a result of emissions of short-lived gases (oxides of nitrogen (NO_x), carbon monoxide and non-methane hydrocarbons) from three transport sectors (ROAD, maritime SHIPping and AIRcraft) are calculated using results from five global atmospheric chemistry models. Using results from these models plus other published data, we quantify the uncertainties. The RF due to short-term O_3 changes (i.e. as an immediate response to the emissions without allowing for the long-term CH_4 changes) is positive and highest for ROAD transport (31 mW m^{-2}) compared to SHIP (24 mW m^{-2}) and AIR (17 mW m^{-2}) sectors in four of the models. All five models calculate negative RF from the CH_4 perturbations, with a larger impact from the SHIP sector than for ROAD and AIR. The net RF of O_3 and CH_4 combined (i.e. including the impact of CH_4 on ozone and stratospheric water vapour) is positive for ROAD ($+16(\pm13)$ (one standard deviation) mW m^{-2}) and AIR ($+6(\pm5)$ mW m^{-2}) traffic sectors and is negative for SHIP ($-18(\pm10)$ mW m^{-2}) sector in all five models. Global Warming Potentials (GWP) and Global Temperature change Potentials (GTP) are presented for AIR NO_x emissions; there is a wide spread in the results from the 5 chemistry models, and it is shown that differences in the methane response relative to the O_3 response drive much of the spread.

1. Introduction

The climate impact of the transport sector occurs through emissions of CO_2, aerosols (and their precursors), water vapour, and species that affect ozone and the oxidative state of the atmosphere such as NO_x, CO and non-methane hydrocarbons (NHMC), with direct emissions of CH_4 being negligible for these sectors. This paper examines the impact of this latter class of oxidant emissions from three transport sub-sectors – land transport (ROAD), maritime shipping (SHIP) and aviation (AIR). We calculate the radiative forcing (RF) by considering both short-term and long-term changes in atmospheric composition. The estimated RF due to all emissions is positive for ROAD and AIR, but negative for SHIP (Fuglestvedt et al., 2008). This switch for SHIP is partly due to the strong direct and indirect aerosol effect from SHIP (Balkanski et al., 2010; Fuglestvedt et al., 2008) but also a result of the high NO_x emissions which reduce the CH_4 lifetime. This coupling in the atmospheric

* Corresponding author. Center for International Climate and Environmental Research-Oslo (CICERO), Oslo, Norway.
E-mail address: gunnar.myhre@cicero.uio.no (G. Myhre).
[1] Now at: International Institute for Applied Systems Analysis, Laxenburg, Austria.

1352-2310/$ – see front matter © 2010 Elsevier Ltd. All rights reserved.
doi:10.1016/j.atmosenv.2010.10.001

chemistry between NO_x, CH_4, and O_3 is well established (Fuglestvedt et al., 1999; Lelieveld et al., 1998; Naik et al., 2005; Shindell et al., 2005, 2009; Wild and Prather, 2000). Emissions of the short-lived trace gas species NO_x, non-methane hydrocarbons (NMHC), and CO lead to production of tropospheric O_3, and we denote this as the short-term O_3 RF. The reduction in CH_4 also leads to additional changes in O_3, but due to the long lifetime of CH_4 compared to the other O_3 precursors, this change in O_3 occurs on a longer time-scale than the short-term O_3 RF (Prather, 1994; Wild et al., 2001). We denote the change in O_3 from CH_4 changes as the CH_4-induced O_3 change.

The RF from O_3 changes since pre-industrial time is estimated to be 0.35 W m^{-2} (Forster et al., 2007; Gauss et al., 2006) and the transport sectors have been estimated to contribute as much as a third of this value (Fuglestvedt et al., 2008). In terms of RF, the reduction in the CH_4 lifetime from NO_x emissions acts on a global scale in opposition to the positive RF due to O_3 production from NO_x, leading to a smaller net effect of NO_x (Forster et al., 2007; Shindell et al., 2005; Wild et al., 2001).

Sector-specific analyses of RF are important, particularly when mitigation measures are being considered because each sector's impact is unique. This is especially relevant for the transport sectors where the emissions are introduced into quite different environments – road emissions are predominantly released into the polluted boundary layer, ship emissions are mostly released into the clean maritime boundary layer, and aircraft emissions are mostly released into the upper troposphere and lower stratosphere. Using several global atmospheric chemistry models and radiative transfer schemes, we quantify the RF resulting from changes in O_3 and the CH_4 lifetime due to emissions of NO_x, CO and NMHCs from the different transport sectors. We focus on the sign of the net RF and its uncertainty for the three transport sectors. The results can be used, together with calculations of the forcing due to other emissions (e.g. CO_2 and black carbon) from the transport sector, to assess and quantify the overall climate impact of each sector (e.g. Skeie et al., 2009).

This paper presents results from the European Union project QUANTIFY (Quantifying the Climate Impact of Global and European Emission Systems). Hoor et al. (2009) reported an analysis of preliminary QUANTIFY simulations, focusing on the behaviour of the different chemical models; they also included a brief discussion of the RF from the different transport sectors. The simulations reported here use the final revised QUANTIFY emission inventories, which were developed during the course of the project (Uherek et al., 2010). We concentrate on a more detailed analysis of the resulting RF and its associated uncertainty and on the computation of climate emissions metrics (Global Warming Potential (GWP) and Global Temperature change Potential (GTP)) for aviation NO_x emissions. An estimate of current climate importance of the accumulated emissions from the transport sector up to year 2000 can be made using RF. To assess the future importance of current emissions and for considerations for mitigation purposes, forward looking emission metrics such as the GWP and the GTP metrics are more useful as they account for the persistence of atmospheric perturbations and thus the integrated impacts (Fuglestvedt et al., 2010).

2. Methods and models

Five global chemistry models consisting of four Chemistry Transport Models (CTMs) and one Climate Chemistry Model (CCM) have been used to simulate changes in O_3 and OH due to precursor emissions (NO_x, CO, and NMHC) from the different transport sectors with year 2000 emissions (see Table 1 for model descriptions). Each model ran with fixed CH_4 abundances and then adopted a spin-up period of a year in order to attain chemical steady state with respect to O_3. The imbalance in the CH_4 budget is diagnosed; this allows the calculation of the change in CH_4 abundance that would have occurred over decades if the emissions were held constant. The QUANTIFY methodology (see Hoor et al., 2009 and Grewe et al., 2010 for details) is to include all natural and anthropogenic emissions and then to compute the impact of an individual transport sector by reducing each respective sector's emissions by 5%, so as to ensure that perturbations act on an atmosphere close to present-day composition (Grewe et al., 2010). The 5% results are scaled by a factor 20 to represent the total change attributable to the transport sectors. The difference between a $20 \times 5\%$ reduction and a complete 100% reduction are discussed in Section 3.1. Fig. 1 compares the improved emissions used in this study compared to those of Fuglestvedt et al. (2008) and Hoor et al. (2009). ROAD emissions of NO_x, NMHC and CO are highest in Fuglestvedt et al. (2008), whereas the new QUANTIFY NO_x emissions for AIR are greater than those in Fuglestvedt et al. (2008) and Hoor et al. (2009). Only Fuglestvedt et al. (2008) included CO and NMHC emissions for the AIR sector, but these emissions are negligible in terms of global anthropogenic sources. Note the much higher ratio of NO_x to CO_2 in SHIP and AIR emissions compared to ROAD emissions. The gridded emission data can be downloaded from www.ip-quantify.eu.

The RF calculations for the O_3 changes from the chemical models are performed using two sets of radiative transfer models, University of Oslo (UiO) and University of Reading (UoR). Except where stated, the simulations here use the UiO schemes, which consist of a broad-band scheme for thermal infrared radiation and a scheme using the multi-stream DISORT code for shortwave radiation (Myhre et al., 2000). UoR have performed O_3 RF calculations using the O_3 changes for each sector averaged over 4 of the global chemistry models (Oslo CTM2, TM4, LMDz-INCA and p-TOMCAT; the UCI results are a recent addition) using the Edwards

Table 1
A short description of the CTMs and CCM used in this study. A more detailed overview of the models is given in Hoor et al. (2009).

Model acronym	Institution	Short description	Reference
Oslo CTM2	University of Oslo, Norway	CTM driven by ECMWF meteorology in T42 horizontal resolution and 60 vertical layers	(Berglen et al., 2004; Gauss et al., 2006; Isaksen et al., 2005)
TM4	KNMI, The Netherlands	CTM driven by ECMWF meteorology with a $2^\circ \times 3^\circ$ horizontal resolution and 34 vertical layers	(van Noije et al., 2006; Williams et al., 2009; Williams et al., 2010)
p-TOMCAT	University of Cambridge, UK	CTM driven by ECMWF meteorology in T21 horizontal resolution and 31 vertical layers	(O'Connor et al., 2005)
LMDz-INCA	LSCE, Gif sur Yvette, France	CCM nudged to meteorological data from ECMWF with a horizontal resolution of $3.75^\circ \times 2.5^\circ$ and 19 vertical layers	(Folberth et al., 2006; Hauglustaine et al., 2004)
UCI	University of California, Irvine, USA	CTM driven by ECMWF meteorology in T42 horizontal resolution and 37 vertical layers	(Hsu et al., 2005; Wild et al., 2003)

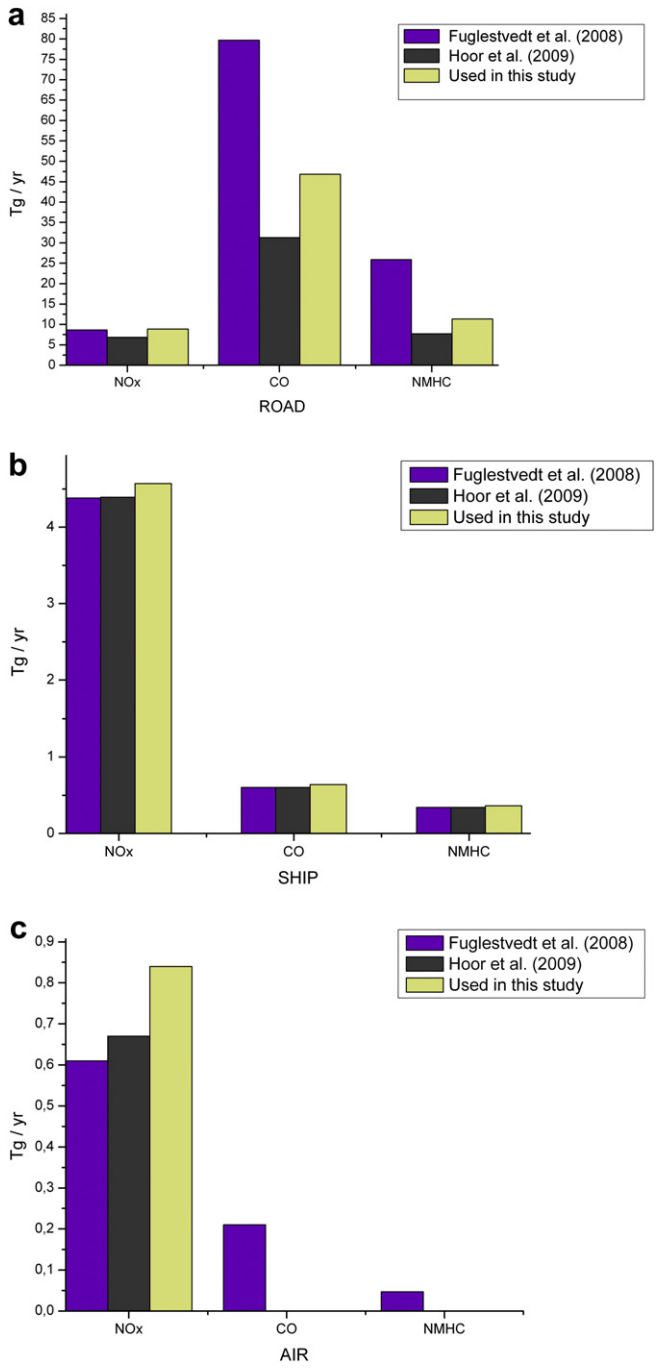

Fig. 1. Emissions (year 2000) of O_3 precursors (NO_x, CO, and NHMC) (given in Tg (N) yr^{-1}, Tg (C) yr^{-1}, and Tg (C) yr^{-1}, respectively) for two previous studies (Fuglestvedt et al., 2008; Hoor et al., 2009) and in this study for ROAD (top), SHIP (middle) and AIR (bottom). For comparison, the CO_2 emissions (as CO_2) in year 2000 are 4200 Tg, 622 Tg and 677 Tg for ROAD, SHIP, and AIR; respectively.

and Slingo (1996) two-stream radiation code, with 6 bands in the shortwave and 8 bands in the longwave.

The methodology for calculating the forcing due to CH_4 changes follows the simple approach described by Berntsen et al. (2005) and used in Hoor et al. (2009), with two important extensions. The chemistry models do not explicitly calculate the change in CH_4 concentrations and in any case the simulations are not long enough for the CH_4 to come into equilibrium with the changed OH field. Instead, the change in OH is used to estimate the fractional change in CH_4 lifetime. This is then multiplied by the present-day concentration of methane and a model-average feedback factor of 1.4 (Prather et al., 2001), to account for the impact of changes in CH_4 concentration on its own lifetime, to yield the fractional change in CH_4 concentration for steady-state conditions (Fuglestvedt et al., 1999). The QUANTIFY study did not directly calculate this feedback factor, nor the increase in tropospheric O_3 per change in CH_4, so we resort to the published, model-average values here.

The RF is calculated assuming a specific CH_4 RF of 0.37 mW $m^{-2}ppbv^{-1}$, which assumes a background concentration of 1740 ppb. The CH_4-induced O_3 RF is then computed, following Berntsen et al. (2005) and using results from Prather et al. (2001), whereby a 10% increase in CH_4 leads to a 0.64 DU increase in O_3, and this O_3 has a specific RF of 42 mW m^{-2} DU^{-1}(Ramaswamy et al., 2001); this RF factor is more applicable to the global-scale change in tropospheric O_3 resulting from the methane change, than it is to the more regional short-term ozone change resulting from transport sector emissions.

The first extension to the Hoor et al. (2009) methodology is to account for the impact of CH_4 changes on stratospheric water vapour. Based on Myhre et al. (2007), we take the stratospheric water vapour RF to be 0.15 times that of the CH_4 RF. The second extension to the Hoor et al. (2009) methodology is to relax the assumption that the CH_4 concentration in 2000 is in steady state with that year's change in OH. The actual degree of imbalance depends on the history of change in OH, which is not accounted for in the chemical model calculations which used year 2000 emissions. The degree of imbalance will be greatest for AIR, for which the emissions have been growing most rapidly in recent years, and least for ROAD. The method and assumptions about the historical emissions are described in Grewe and Stenke (2008). The factor to correct this transient response in year 2000 is taken to be 0.85 for ROAD, 0.8 for SHIP and 0.65 for AIR. These factors are then applied to the CH_4 RF, the CH_4-induced O_3 RF and the stratospheric water vapour RF from each of the CTMs. These corrections to the instantaneous year 2000 RF are a result of the historical emissions and do not apply to the calculation of GWP and GTP for AIR in Section 4.

Other consequences of the O_3 precursor emissions have been identified but are not considered here. For example, changes in O_3 and OH may alter the sulphate burden (e.g. Unger et al., 2006; Shindell et al., 2009) and surface O_3 interaction with vegetation may impact the carbon cycle (Sitch et al., 2007). NO_x emissions have a small direct RF due to the absorption of solar radiation by NO_2 (Kvalevåg and Myhre, 2007) and formation of nitrate aerosols from the NO_x enhances the overall aerosol negative RF (Forster et al., 2007). This paper focuses on the primary, well-established impacts of the ozone-precursor emissions on O_3 and CH_4 and their consequential effects.

3. Results

3.1. Short-term O_3

Table 2 compares the global and annual mean total column O_3 change (in DU) for the five global chemistry models and the three transport sectors for the QUANTIFY preliminary emissions (Hoor et al., 2009) and QUANTIFY final emissions used here. The largest changes in the O_3 column between the simulations using the preliminary and final emissions are seen for ROAD and AIR. In addition to changes in the emissions inventories, there have also been model improvements and updates by many of the modelling groups over the two-year period in which the QUANTIFY emissions were updated. p-TOMCAT is the only model with a reduction in the O_3 column change for all three transport sectors between

Table 2
The short-term global and annual mean O_3 column change (in DU) for the five models and the year 2000 emissions from the three transport sectors for both the QUANTIFY preliminary emissions (Hoor et al., 2009) and the QUANTIFY final emissions (this study).

	Oslo CTM2		TM4		p-TOMCAT		LMDz-INCA		UCI	
	Preliminary	Final	Preliminary	Final	Preliminary	Final	Preliminary	Final	Preliminary	Final
ROAD	0.99	1.38	0.72	0.88	0.59	0.51	0.77	0.94	0.80	1.25
SHIP	0.96	1.02	0.71	0.68	0.82	0.65	0.67	0.55	0.84	1.04
AIR	0.30	0.48	0.32	0.43	0.70	0.51	0.35	0.39	0.35	0.63

preliminary and final QUANTIFY simulations in spite of increased NO_x emissions.

Fig. 2 shows the global and annual mean RF for short-term O_3, using the UiO radiation model, for the three transport sectors calculated by the five global chemistry models. Amongst the transport sectors, ROAD is largest, followed by SHIP and AIR sectors in four of the models. The five model average for the ROAD, SHIP and AIR sectors are 31, 24 and 17 mW m^{-2}, respectively. A composite, four model (without UCI) mean of the O_3 change is used to compare the radiation models. For this subset the UiO RF values are 30, 21 and 16 mW m^{-2} for the three sub-sectors, and the UoR calculations yield corresponding forcings of 28, 19 and 17 mW m^{-2} indicating agreement to within about 10% in the RF calculations.

The relative spread in the RF among the models is within a factor of 2 for AIR, (13–21 mW m^{-2}) and SHIP (17–32 mW m^{-2}); by contrast for ROAD the spread in the RF is almost a factor of 3 (15–42 mW m^{-2}). The model range in the sum of RF across all three sectors is less and ranges from 57 to 90 mW m^{-2}.

The zonal-mean RFs of short-term O_3 for the three transport sectors for all five models are shown in Fig. 3. The patterns of RF are similar for the four models Oslo CTM2, TM4, LMDz-INCA, and UCI, as governed by the global distribution of emissions for each sector, with ROAD dominating in the Northern Hemisphere, ROAD and SHIP being quite comparable in the Southern Hemisphere, and AIR being very small in the Southern Hemisphere. By contrast, the p-TOMCAT RF shows AIR as dominating in the Northern Hemisphere and comparably large also in the Southern Hemisphere.

The RF results are based on radiation calculations using the 100% perturbation in O_3 that is derived by multiplying the ozone change resulting from the 5% perturbation in emissions by 20 (Grewe et al., 2010; Hoor et al., 2009). Hoor et al. (2009) showed that the sum of O_3 changes from 5% perturbation in the individual ROAD, AIR and SHIP emissions equals that from a single calculation of the combined emissions from all three sectors. Here, we investigate the difference between a scaled 5% reduction and a full 100% reduction of ROAD emissions with the Oslo CTM2: the 100% reduction gives column O_3 changes that are 1.07 times greater than 20 × 5%; however, the non-linearity in the longwave RF reduces this to a factor of 1.03. Compared to the inter-model differences in the RF, the non-linear response to the magnitude of the perturbations is relatively small, and hence contributes little to the overall uncertainty.

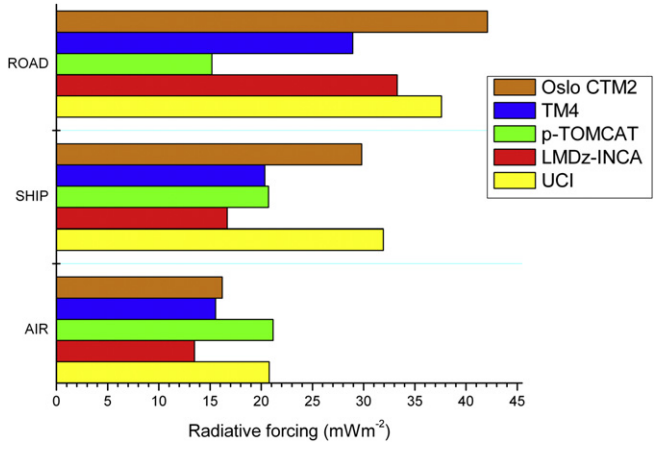

Fig. 2. Global and annual mean radiative forcing due to short-term O_3 (mW m^{-2}) for year 2000 emissions from three transport sectors and five global chemistry models, as calculated using the UiO radiation schemes.

Normalized radiative forcing from O_3 (NRF) (RF divided by the change in the O_3 column expressed in Dobson Units (DU)) is dependent on both the region and altitude of the resulting O_3 change (Berntsen et al., 2000; Gauss et al., 2003). In all models, except LMDz-INCA, the AIR sector has a higher NRF than ROAD and SHIP with a mean of 36 mW m^{-2} DU^{-1} with a range from 33 to 42 mW m^{-2} DU^{-1}. The values for ROAD and SHIP are 32 mW m^{-2} DU^{-1} (range from 30 to 36 mW m^{-2} DU^{-1}) and 30 mW m^{-2} DU^{-1} (range from 29 to 32 mW m^{-2} DU^{-1}), respectively. For the sum of RF across the three transport sectors, p-TOMCAT yields the highest NRF (34 mW m^{-2} DU^{-1}) and Oslo CTM2 the lowest (31 mW m^{-2} DU^{-1}). These NRF numbers show the largest spread for AIR. In some instances the agreement in the RF between models is a coincidence resulting from compensating differences in the NRF and the ozone change (as is the case for p-TOMCAT and UCI for AIR). Nevertheless, these comparisons in NRF show much less relative spread compared to the RF calculations, indicating that it is inter-model differences in the total O_3 change that are mainly responsible for the differences in their RF, rather than inter-model differences in the distribution of the O_3 change.

3.2. CH_4

The O_3 precursor emissions change the atmospheric lifetime of CH_4 due to changes in OH concentrations. The percentage changes in the CH_4 lifetime due to destruction by OH (integrated between the surface and 50 hPa for each model) are given in Table 3. For most models and most transport sectors, increased emissions lead to an increase in global OH, a decrease in CH_4 lifetime and hence a decrease in CH_4 concentrations. The changes are largest for SHIP because of the different geographical pattern of emissions and background conditions as well as the mix of emitted components compared to the other sectors (Fuglestvedt et al., 2008; Hoor et al., 2009). Although AIR emissions have the largest impact on CH_4 on a per unit NO_x emission basis, SHIP and ROAD each have nearly ten times larger NO_x emissions. Unlike the results in Hoor et al. (2009), where all models (including p-TOMCAT) and all sectors showed a decrease in CH_4 lifetime, the current p-TOMCAT version using the final QUANTIFY emissions calculates a small increase in CH_4 lifetime for ROAD. Our analysis finds that p-TOMCAT has a much stronger response of the OH concentrations to emissions of CO and NMHC than the other models and this overwhelms the effect of the NO_x emissions. This model has lower CO concentrations than the four other models, which can partly explain the different impact of the ROAD emissions.

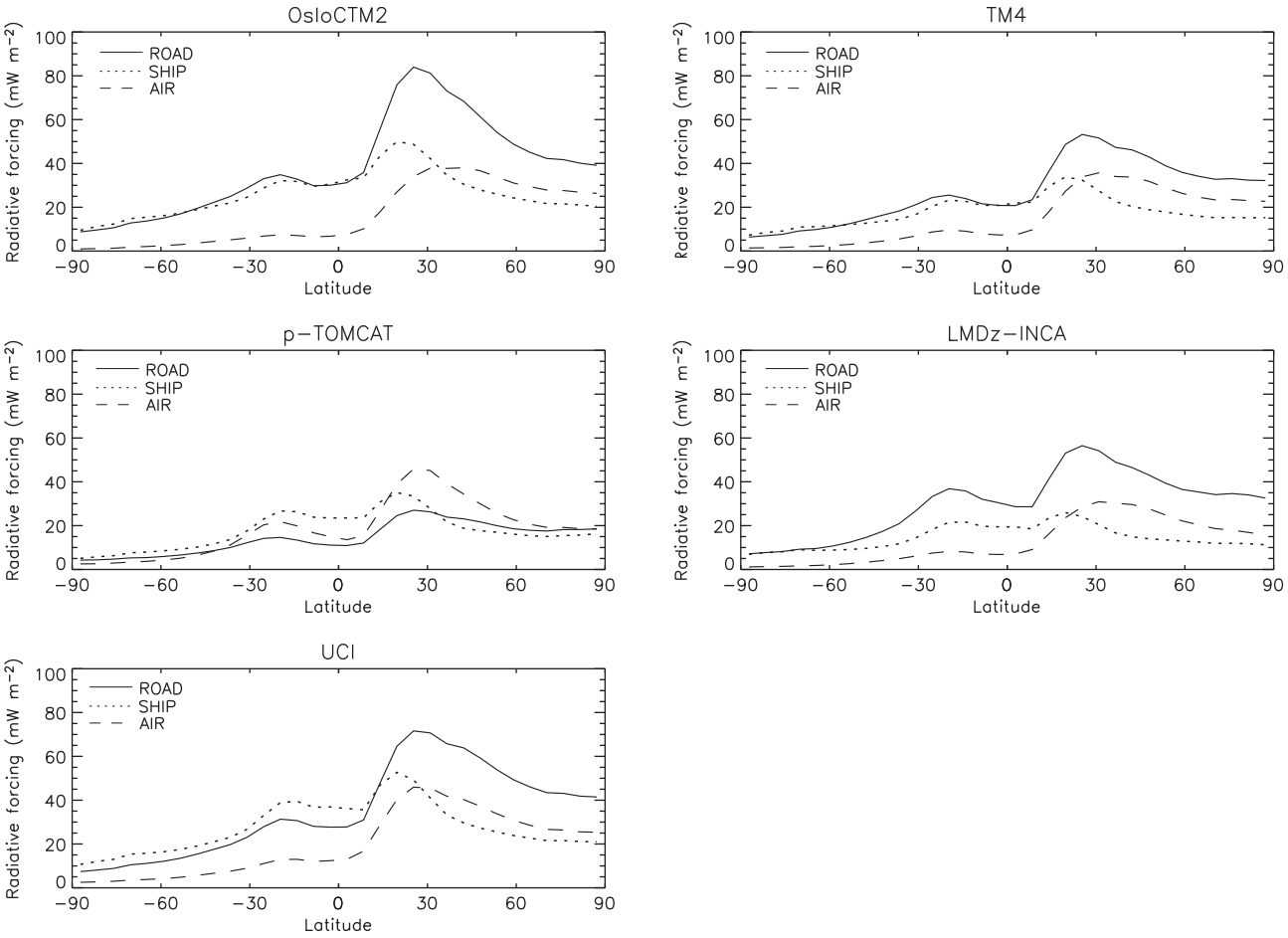

Fig. 3. Zonal and annual mean radiative forcing (mW m^{-2}) from short-term O_3 for five global chemistry models. Each panel shows results for year 2000 emissions from three transport sectors.

The resulting RF for year 2000 due to CH_4 change from the transport sector (including the transient effect but not the CH_4-induced changes in O_3 and stratospheric water vapour) is shown in Fig. 4. This CH_4 RF is larger for SHIP than ROAD and AIR. The inter-model difference in the CH_4 RF is rather small for SHIP, with a spread of only 8 mW m^{-2} for an average RF of −27 mW m^{-2}. For AIR, all models show a negative RF, with a mean of −7.3 mW m^{-2} and a relatively higher spread of 4.4 mW m^{-2}. The ROAD RF from CH_4 varies little among four global models, −12 to −14 mW m^{-2}, but p-TOMCAT gives +1 mW m^{-2}, reducing the magnitude of the mean RF for ROAD for the CH_4 lifetime to −10 mW m^{-2}.

3.3. RF due to short-term O_3 and CH_4 changes combined

The net RF of short-term O_3 and long-term CH_4 combined (and now including the CH_4 impacts on O_3 and stratospheric water vapour) are shown in Fig. 5. All five models have a positive net RF for ROAD and AIR and a negative RF for SHIP. For ROAD, the net forcing varies from 9.3 to 21 mW m^{-2}, with a mean of 16 mW m^{-2}. For SHIP, the range is −12 to −25 mW m^{-2} with a mean of −18 mW m^{-2}. Although the general agreement in Fig. 5 is quite encouraging in terms of absolute RF, the degree of agreement is less

Table 3
CH_4 lifetimes (yr) due to destruction by OH (between the surface and 50 hPa) for the base case and the relative changes due to year 2000 emissions from three transport sectors – the values are derived from a 5% change in emissions for each sector and then multiplied by 20. The feedback effect of changes in CH_4 on its own lifetime is not included in this Table.

	Oslo CTM2	TM4	p-TOMCAT	LMDz-INCA	UCI
Base (years)	8.29	8.59	9.38	9.02	7.81
Road %	−1.77	−1.62	0.12	−1.54	−1.78
Ship %	−3.74	−4.14	−3.45	−3.14	−4.24
Air %	−0.81	−1.22	−1.55	−1.04	−1.57

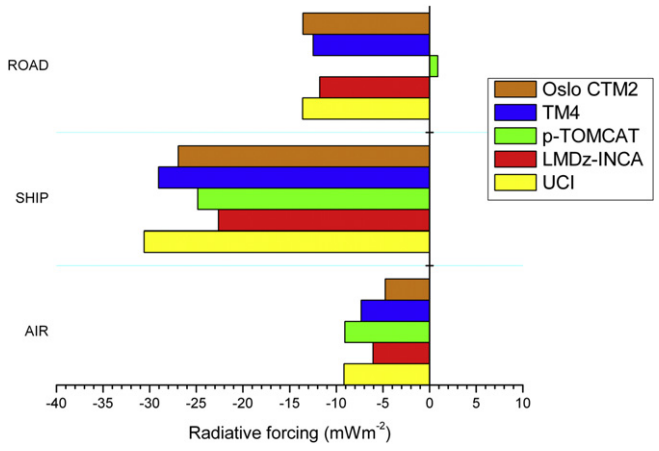

Fig. 4. Global and annual mean radiative forcing for the year 2000 due to CH_4 changes (mW m^{-2}) accounting for the time-history of the emissions (see text for details) for three transport sectors and five global chemistry models.

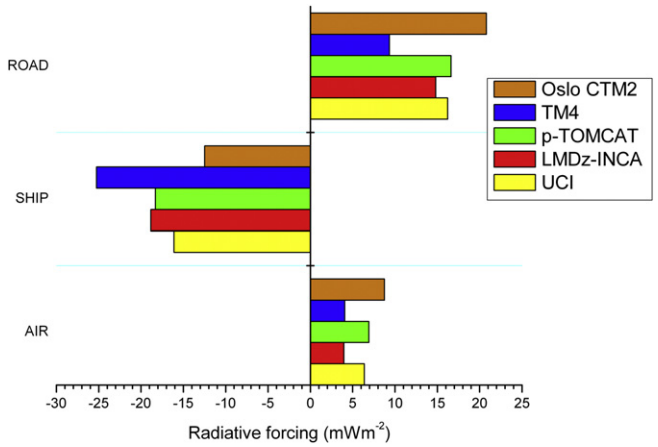

Fig. 5. Net RF of O_3 and CH_4 (including stratospheric water vapour) in year 2000 accounting for the time-history of the emissions (see text for details) for three transport sectors and five global chemistry models.

than that seen in Fig. 4 (p-TOMCAT for ROAD excepted). This is because the models show a differing amount of cancellation between the short-term O_3 RFs and CH_4. This uncertainty in the long-term RF (CH_4 plus induced O_3 changes) may be underestimated since we used a single conversion factor for the CH_4 feedback on its own lifetime, and a single factor for the RF due to the CH_4-induced ozone change and the stratospheric H_2O change. For AIR, the spread is from 4.1 to 8.7 mW m^{-2} with a mean of 6.0 mW m^{-2}. Compared to the multi-model mean, Oslo CTM2 is always more positive, by several 10's of percent, TM4 is always more negative by several tens of percent, while deviations from the mean for LMDz-INCA, UCI and p-TOMCAT are generally smaller and all are within 10% of the multi-model mean for two of the three sectors.

To derive the uncertainties in the RF, we use uncertainties in the emissions (Fuglestvedt et al., 2008), and simulations of distribution changes and radiative forcing performed in this study combined with Monte Carlo simulations (Boucher and Haywood, 2001). For O_3 and the CH_4 lifetime effect we use the difference in the global chemistry models as one standard deviation representative for the uncertainty in distributions for each of the transport sectors. The uncertainty in the CH_4 impact on O_3 takes into account uncertainty in the model change in CH_4 and O_3 in addition to the uncertainty in emissions. For stratospheric water vapour uncertainties in the emissions, CH_4 change and the radiative transfer are considered. The latter is taken from an intercomparison study with an uncertainty of 30% (Myhre et al., 2009). The derived uncertainties (one standard deviation) are 13 mW m^{-2} (81%), 10 mW m^{-2} (55%), and 5 mW m^{-2} (81%) for ROAD, SHIP, and AIR, respectively. The dominating contributor to the uncertainty is the short-term O_3.

4. Climate emission metrics for aviation NO_x emissions

Fuglestvedt et al. (2010) reported values (as well as a number of important caveats) for the GWP and GTP for NO_x emissions from aviation using available results in the literature. They found substantial differences in the derived GWPs and GTPs, which included a difference in sign for some time horizons (H). The results derived here allow a cleaner comparison of GWPs and GTPs between global chemistry models, as they are derived using the same emissions and emission perturbations, the same experimental design and use the same radiative transfer scheme to calculate the RF. Thus the spread in results gives us a measure of the uncertainty in the global chemical modelling of aviation's impact on atmospheric chemistry. We do not present values for the other sectors, as the ozone changes for these are influenced by CO and NMHC emissions as well as NO_x.

The Fuglestvedt et al. (2010) methodology is adopted here for the calculation of GWPs and GTPs, although we also include the effect of CH_4 changes on stratospheric water vapour. In line with the conventional definitions of GWP and GTP, CO_2 is used as the reference gas. The GTP values are somewhat sensitive to the model used to calculate the temperature change, and the assumed climate sensitivity. Appendix 2 in Fuglestvedt et al. (2010) describes the method used here, which is based on fits to coupled ocean-atmosphere general circulation model experiments, which have an equilibrium climate sensitivity to a doubling of CO_2 of 3.9 K. The CH_4 lifetimes given in Table 3 are multiplied by 1.4 to give the CH_4 perturbation lifetimes (which accounts for the effect of a change in CH_4 on its own lifetime). Table 4 shows the specific RFs (in W m^{-2} (kgN yr^{-1})) for the short-lived ozone, methane-induced ozone and methane for the 5 models, as well as the multi-model mean, which are required as input to the GWP and GTP calculations.

The resulting GWP values for three time horizons ($H = 20$, 100 and 500 years) are shown in Table 5a, and for the GTPs (H = 20, 50 and 100 years), in Table 5b. In both tables, the values are split into three components – the short-term O_3 effect resulting directly from the NO_x emissions, the decadal CH_4-induced O_3 change and the CH_4 change itself, which is scaled to include the stratospheric water vapour effect (which is 0.15 of the direct effect). The range of results given in Fuglestvedt et al. (2010) is also shown. Considering the GWP, the results indicate at first sight that the range from the present models – an indicator of the uncertainty in the GWP – is no smaller than that derived in Fuglestvedt et al. (2010). For $H = 20$ years, there is a spread of a factor of 3; for $H = 100$ and 500 years, the different models do not even agree in sign. For GTP, the situation is similar: for $H = 20$ and 50 years, the spread is no less than in Fuglestvedt et al. (2010), while for $H = 100$ years, there is disagreement in sign.

However, Table 5 reveals important patterns that give hope that the reasons for the model differences can be resolved. For all metrics and all time horizons, values from the Oslo CTM2 are clearly the most positive (as is true also for the net forcings for all sectors shown in Fig. 5); for GWP ($H = 20$), GWP ($H = 100$) and GTP ($H = 100$) it is the *only* model generating a positive value. Removing the Oslo CTM2 model, markedly reduces the range in both the GWPs and GTPs. For example GWP ($H = 100$) changes from −21 to 67, to −21 to −6.3; and GTP ($H = 100$) changes from −5.8 to 7.9 to −5.8 to −4.6. Much less markedly, TM4 is the most negative for all GWP time horizons, and p-TOMCAT is generally the most negative for GTP ($H = 50$) and GTP($H = 100$).

This behaviour seems largely a result of one characteristic of the models – the ratio of the percentage change in CH_4 lifetime to the O_3 column change. Using Tables 2 and 3, the values for AIR range from −1.7% DU^{-1} for Oslo CTM2, −2.8% DU^{-1} for TM4, −2.5% DU^{-1} for UCI, −2.7% DU^{-1} for LMDz-INCA to −3.0% DU^{-1} for p-TOMCAT.

Table 4
Steady-state radiative forcings (in W m^{-2} (kgN yr^{-1})) for sustained AIR NO_x emissions for each of the 5 models and the mean of the 5 models. In this table, for example, 1.94E-11 denotes 1.94×10^{-11} etc.

	Short-lived ozone	Methane-induced ozone	methane
Oslo CTM2	1.94E-11	−3.68E-12	−1.01E-11
TM4	1.86E-11	−5.52E-12	−1.51E-11
p-TOMCAT	2.54E-11	−7.02E-12	−1.92E-11
LMDz-INCA	1.62E-11	−4.69E-12	−1.29E-11
UCI	2.49E-11	−7.10E-12	−1.94E-11
Mean	2.09E-11	−5.60E-12	−1.53E-11

Table 5
Global Warming Potentials (GWP) and Global Temperature change Potentials (GTP) for year 2000 AIR NO_x emissions (a) GWP values for one-year pulse emissions of NO_x for a 20, 100 and 500 year time horizons and (b) GTP values for 20, 50 and 100 years. The first three numbers show the individual contributions from the short-lived O_3, the CH_4-induced O_3 and the CH_4 (which includes stratospheric water vapour changes), respectively; the net GWP and GTP are shown in bold. The mean values use the multi-model means of the specific forcings (Table 4) and lifetimes (Table 3). All numbers are rounded, so that the net values may not be the sum of numbers as they are presented here. All values are on a per kg N basis and are relative to CO_2. The GTP values are specific to a given value of climate sensitivity – see text for details.

(a) GWP	$H = 20$	$H = 100$	$H = 500$
Oslo CTM2	785 − 115 − 333 = **338**	223 − 41 − 116 = **67**	68 − 12 − 5 = **20**
TM4	753 − 170 − 490 = **92**	214 − 61 − 174 = **−21**	65 − 19 − 53 = **−6.3**
p-TOMCAT	1028 − 209 − 601 = **218**	292 − 78 − 221 = **−6.3**	89 − 24 − 67 = **−2.0**
LMDz-INCA	656 − 142 − 411 = **103**	186 − 52 − 148 = **−14**	57 − 16 − 45 = **−4.2**
UCI	1008 − 226 − 654 = **128**	287 − 78 − 223 = **−15**	87 − 24 − 68 = **−4.5**
Mean	846 − 173 − 496 = **177**	241 − 62 − 176 = **2.7**	73 − 19 − 54 = **0.8**
Range of net	92 to 338	−21 to 67	−6.3 to 20
Fuglestvedt et al. (2010) range of net	120 to 470	−2.1 to 71	−0.7 to 22
(b) GTP	$H = 20$	$H = 50$	$H = 100$
Oslo CTM2	248 − 271 − 97 = **−121**	39 − 55 − 20 = **−37**	32 − 18 − 6.2 = **7.9**
TM4	238 − 406 − 145 = **−313**	37 − 87 − 31 = **−81**	30 − 27 − 9.4 = **−5.6**
p-TOMCAT	324 − 510 − 183 = **−369**	51 − 122 − 44 = **−115**	41 − 35 − 12.3 = **−5.8**
LMDz-INCA	206 − 343 − 123 = **−259**	32 − 78 − 28 = **−74**	26 − 23 − 8.1 = **−4.7**
UCI	318 − 526 − 188 = **−396**	50 − 100 − 36 = **−86**	41 − 34 − 11.7 = **−4.6**
Mean	267 − 412 − 147 = **−292**	42 − 88 − 32 = **−79**	34 − 27 − 9.5 = **−4.1**
Range of net	−396 to −121	−115 to −37	−5.8 to 7.9
Fuglestvedt et al. (2010) range of net	−590 to −200	−210 to −59	−9.5 to 7.6

Hence, for the Oslo CTM2 model the compensating effect of the negative forcing due to CH_4 and its resulting effect on stratospheric water vapour and O_3 is smaller than for the other models. The differences in CH_4 lifetime between the models (Table 4) have only a small influence on the range of results.

If the reason why the models differ in ratio of CH_4 change to O_3 change can be understood, there is hope for a marked reduction in the inter-model range in the estimated net RF from transport and in metrics such as the GWP and GTP. However, as is clear in Table 5, even when models agree in the net value of a metric, the individual components contributing to this net value can be quite different – for example, UCI and p-LMDz-INCA agree well in the net for both metrics and most time horizons, but disagree significantly for the three components; this effect is traceable to the larger change in O_3 in UCI compared to LMDz-INCA (see Table 2).

5. Conclusions

We have investigated the RF for the year 2000 due to changes in O_3 and CH_4 caused by the transport sector, using five global chemistry models and two radiation models. We find the difference between ROAD, SHIP and AIR to be robust across all models. For the year 2000, this study reduces the CH_4 and CH_4-induced O_3 impacts to account for the slower response of CH_4 perturbations to changes in OH. It also includes the effect of CH_4 changes on stratospheric water vapour. The results are also used to present values of GWP and GTP for AIR NO_x emissions which are based on a range of global chemistry models adopting the same experimental design.

Fuglestvedt et al. (2008) found, based on one global chemistry transport model and one radiative transfer model, a year 2000 RF for the combined effect of O_3 and CH_4 amounting to 42 mW m^{-2} for ROAD, −11 mW m^{-2} for SHIP and 12 mW m^{-2} for AIR, based on a different set of emissions (see Fig. 1). The multi-model means obtained here are 16 mW m^{-2}, −18 mW m^{-2} and 6.0 mW m^{-2} respectively. The ROAD and AIR are significantly smaller in the present analysis than in (Fuglestvedt et al., 2008), while SHIP is significantly more negative. Various factors explain the differences. First, the emissions are different. As a consequence, a lower ozone production (at least for ROAD with lower CO and NHMC emissions) and hence less net positive radiative forcing is calculated. Second, the secondary consequences of methane changes included here (i.e. responses in O_3 and stratospheric H_2O) increase the negative radiative forcings. Third, the Oslo CTM2, which was used in the Fuglestvedt et al. (2008) study is seen here to produce results at the upper end of the spectrum, compared with the multi-model mean. All three factors act together to lower the calculated radiative forcing from the transport sectors compared to the values in Fuglestvedt et al. (2008). The RF for the combined effect of O_3 and CH_4 can be compared to the RF due to CO_2 which has previously been estimated to be 150 mW m^{-2}, 35 mW m^{-2}, 21 mW m^{-2} for ROAD, SHIP, and AIR, respectively (Fuglestvedt et al., 2008).

The results reported here with the QUANTIFY inventories can be compared with the previous Hoor et al. (2009) results using preliminary QUANTIFY inventories, where the multi-model means were 7.3 mW m^{-2}, −26 mW m^{-2} and 2.9 mW m^{-2} for ROAD, SHIP and AIR, respectively. For SHIP and AIR part of the difference is due to account being taken here of the lack of steady state of the CH_4 field with the changed OH field, which reduces the size of the CH_4 offset to the positive short-term O_3 forcing. The factor of more than two change for ROAD has a number of identified reasons (emissions, model updates, and method for CH_4 RF calculations); the short-term O_3 forcing is only changed by about 10% while the offset resulting from the changed OH field is now smaller. Based on the much higher emissions of CO and NMHC in Fuglestvedt et al. (2008) it is expected that the O_3 RF for ROAD was higher in that study compared to Hoor et al. (2009) and this study (see Fig. 1). On robustness and uncertainties for road transport, the O_3 RF is highly dependent on the background NO_x emissions used in the model, including those from power generation, agriculture, lightning and biomass burning.

The inter-model absolute differences are smaller when the combined effects of O_3 and CH_4 RFs are calculated than they are for the, short-term O_3 RF alone. Nevertheless, the combined O_3 and CH_4 RF from individual models can deviate by many tens of percent from the multi-model mean. One significant factor in these differences, and the difference in the aviation climate emission metrics, is the ratio of the percentage change in CH_4 lifetime to the column O_3 change. If the underlying reasons for this ratio could be understood, there is the possibility of markedly decreasing the inter-model differences.

The RF resulting from the effect of transport-related emissions on ozone and methane reported here must be combined with estimates of the transport-related RF from aerosols and CO_2 (e.g. Balkanski et al., 2010) to improve understanding of the overall impact of the transport sector on climate.

Acknowledgements

The QUANTIFY project is funded by the European Union within the 6th Framework Programme under contract 003893 and the Norwegian Research Council. The reviewers are thanked for their helpful comments.

References

Balkanski, Y., Myhre, G., Gauss, M., Rädel, G., Highwood, E.J., et al., 2010. Direct radiative effect of aerosols emitted by transport: from road, shipping and aviation. Atmos. Chem. Phys. 10, 4477–4489.

Berglen, T.F., Berntsen, T.K., Isaksen, I.S.A., Sundet, J.K., 2004. A global model of the coupled sulfur/oxidant chemistry in the troposphere: the sulfur cycle. J. Geophys. Res. 109 (D19), D19310. doi:10.1029/2003JD003948.

Berntsen, T.K., Fuglestvedt, J.S., Joshi, M.M., Shine, K.P., Stuber, N., et al., 2005. Response of climate to regional emissions of ozone precursors: sensitivities and warming potentials. Tellus 57 (4), 283–304.

Berntsen, T.K., Myhre, G., Stordal, F., Isaksen, I.S.A., 2000. Time evolution of tropospheric ozone and its radiative forcing. J. Geophys. Res. 105 (D7), 8915–8930.

Boucher, O., Haywood, J., 2001. On summing the components of radiative forcing of climate change. Clim. Dynam. 18 (3–4), 297–302.

Edwards, J.M., Slingo, A., 1996. Studies with a flexible new radiation code. I: Choosing a configuration for a large-scale model. Q.J.R. Meteorol.Soc. 122, 689–719.

Folberth, G.A., Hauglustaine, D.A., Lathiere, J., Brocheton, F., 2006. Interactive chemistry in the Laboratoire de Meteorologie Dynamique general circulation model: model description and impact analysis of biogenic hydrocarbons on tropospheric chemistry. Atmos. Chem. Phys. 6, 2273–2319.

Forster, P., Ramaswamy, V., Artaxo, P., Berntsen, T., Betts, R., et al., 2007. Changes in atmospheric constituents and in radiative forcing. In: Solomon, S., Qin, D., Manning, M., Chen, Z., Marquis, M., et al. (Eds.), Climate Change 2007: The Physical Science Basis. Contribution of Working Group I to the Fourth Assessment Report of the Intergovernmental Panel on Climate Change. Cambridge University Press, United Kingdom and New York, NY, USA.

Fuglestvedt, J., Berntsen, T., Myhre, G., Rypdal, K., Skeie, R.B., 2008. Climate forcing from the transport sectors. Proc. Natl. Acad. Sci. U S A 105 (2), 454–458.

Fuglestvedt, J.S., Berntsen, T.K., Isaksen, I.S.A., Mao, H.T., Liang, X.Z., et al., 1999. Climatic forcing of nitrogen oxides through changes in tropospheric ozone and methane; global 3D model studies. Atmos. Environ. 33 (6), 961–977.

Fuglestvedt, J.S., Shine, K.P., Cook, J., Berntsen, T., Lee, D.S., et al., 2010. Assessment of transport impacts on climate and ozone: metrics. Atmos. Environ. 44, 4648–4677. doi:10.1016/j.atmosenv.2009.04.044.

Gauss, M., Myhre, G., Isaksen, I.S.A., Grewe, V., Pitari, G., et al., 2006. Radiative forcing since preindustrial times due to ozone change in the troposphere and the lower stratosphere. Atmos. Chem. Phys. 6, 575–599.

Gauss, M., Myhre, G., Pitari, G., Prather, M.J., Isaksen, I.S.A., et al., 2003. Radiative forcing in the 21st century due to ozone changes in the troposphere and the lower stratosphere. J. Geophys. Res. 108 (D9), 4292.

Grewe, V., Stenke, A., 2008. AirClim: an efficient tool for climate evaluation of aircraft technology. Atmos. Chem. Phys. 8 (16), 4621–4639.

Grewe, V., Tsati, E., Hoor, P., 2010. On the attribution of contributions of atmospheric trace gases to emissions in atmospheric model applications. Geosci. Model Dev. 3, 487–499.

Hauglustaine, D.A., Hourdin, F., Jourdain, L., Filiberti, M.A., Walters, S., et al., 2004. Interactive chemistry in the Laboratoire de Meteorologie Dynamique general circulation model: description and background tropospheric chemistry evaluation. J. Geophys. Res. 109 (D4), D04314.

Hoor, P., Borken-Kleefeld, J., Caro, D., Dessens, O., Endresen, O., et al., 2009. The impact of traffic emissions on atmospheric ozone and OH: results from QUANTIFY. Atmos. Chem. Phys. 9 (9), 3113–3136.

Hsu, J., Prather, M.J., Wild, O., 2005. Diagnosing the stratosphere-to-troposphere flux of ozone in a chemistry transport model. J. Geophys. Res. 110 (D19), D19305.

Isaksen, I.S.A., Zerefos, C., Kourtidis, K., Meleti, C., Dalsoren, S.B., et al., 2005. Tropospheric ozone changes at unpolluted and semipolluted regions induced by stratospheric ozone changes. J. Geophys. Res. 110 (D2), D02302.

Kvalevåg, M.M., Myhre, G., 2007. Human impact on direct and diffuse solar radiation during the industrial era. J. Clim. 20 (19), 4874–4883.

Lelieveld, J., Crutzen, P.J., Dentener, F.J., 1998. Changing concentration, lifetime and climate forcing of atmospheric methane. Tellus 50 (2), 128–150.

Myhre, G., Karlsdottir, S., Isaksen, I.S.A., Stordal, F., 2000. Radiative forcing due to changes in tropospheric ozone in the period 1980 to 1996. J. Geophys. Res. 105 (D23), 28935–28942.

Myhre, G., Kvalevag, M., Radel, G., Cook, J., Shine, K.P., et al., 2009. Intercomparison of radiative forcing calculations of stratospheric water vapour and contrails. Meteorol. Z. 18 (6), 585–596.

Myhre, G., Nilsen, J.S., Gulstad, L., Shine, K.P., Rognerud, B., et al., 2007. Radiative forcing due to stratospheric water vapour from CH_4 oxidation. Geophys. Res. Lett. 34 (1), L01807.

Naik, V., Mauzerall, D., Horowitz, L., Schwarzkopf, M.D., Ramaswamy, V., et al., 2005. Net radiative forcing due to changes in regional emissions of tropospheric ozone precursors. J. Geophys. Res. 110 (D24), D24306.

O'Connor, F., Carver, G., Savage, N., Pyle, J., Methven, J., et al., 2005. Comparison and visualisation of high-resolution transport modelling with aircraft measurements. Atmos. Sci. Lett. 6, 164–170. doi:10.1002/asl.111.

Prather, M., Ehhalt, D., Dentener, F., Derwent, R., Dlugokencky, E., et al., 2001. Atmospheric chemistry and greenhouse gases. e. a.. In: Houghton, J.T. (Ed.), Climate Change 2001: The Scientific Basis, Contribution of Working Group I to the Third Assessment Report of the Intergovernmental Panel on Climate Change. Cambridge University Press, Cambridge, United Kingdom and New York, NY, USA, pp. 239–287.

Prather, M.J., 1994. Lifetimes and eigenstates in atmospheric chemistry. Geophys. Res. Lett. 21 (9), 801–804.

Ramaswamy, V., Boucher, O., Haigh, J., Hauglustaine, D., Haywood, J., et al., 2001. Radiative forcing of climate change. In: Houghton, J.T., et al. (Eds.), Climate Change 2001: The Scientific Basis, Contribution of Working Group I to the Third Assessment Report of the Intergovernmental Panel on Climate Change. Cambridge University Press, Cambridge, United Kingdom and New York, NY, USA, pp. 349–416.

Shindell, D.T., Faluvegi, G., Bell, N., Schmidt, G.A., 2005. An emissions-based view of climate forcing by methane and tropospheric ozone. Geophys. Res. Lett. 32 (4), L04803.

Shindell, D.T., Faluvegi, G., Koch, D.M., Schmidt, G.A., Unger, N., et al., 2009. Improved attribution of climate forcing to emissions. Science 326 (5953), 716–718.

Sitch, S., Cox, P.M., Collins, W.J., Huntingford, C., 2007. Indirect radiative forcing of climate change through ozone effects on the land-carbon sink. Nature 448 (7155), 791–794.

Skeie, R.B., Fuglestvedt, J., Berntsen, T., Lund, M.T., Myhre, G., et al., 2009. Global temperature change from the transport sectors: historical development and future scenarios. Atmos. Environ. 43 (39), 6260–6270.

Uherek, E., Halenka, T., Borken-Kleefeld, J., Balkanski, Y., Berntsen, T., et al., 2010. Transport impacts on atmosphere and climate: land transport. Atmos. Environ. 44, 4772–4816.

Unger, N., Shindell, D.T., Koch, D.M., Amann, M., Cofala, J., et al., 2006. Influences of man-made emissions and climate changes on tropospheric ozone, methane, and sulfate at 2030 from a broad range of possible futures. J. Geophys. Res. 111 (D12), D12313.

van Noije, T.P.C., Eskes, H.J., Dentener, F.J., Stevenson, D.S., Ellingsen, K., et al., 2006. Multi-model ensemble simulations of tropospheric NO_2 compared with GOME retrievals for the year 2000. Atmos. Chem. Phys. 6, 2943–2979.

Wild, O., Prather, M.J., 2000. Excitation of the primary tropospheric chemical mode in a global three-dimensional model. J. Geophys. Res. 105 (D20), 24647–24660.

Wild, O., Prather, M.J., Akimoto, H., 2001. Indirect long-term global radiative cooling from NO_x emissions. Geophys. Res. Lett. 28 (9), 1719–1722.

Wild, O., Sundet, J.K., Prather, M.J., Isaksen, I.S.A., Akimoto, H., et al., 2003. Chemical transport model ozone simulations for spring 2001 over the western Pacific: comparisons with TRACE-P lidar, ozonesondes, and Total Ozone Mapping Spectrometer columns. J. Geophys. Res. 108 (D21), 8826.

Williams, J.E., Scheele, M.P., van Velthoven, P.F.J., Cammas, J.P., Thouret, V., et al., 2009. The influence of biogenic emissions from Africa on tropical tropospheric ozone during 2006: a global modeling study. Atmos. Chem. Phys. 9 (15), 5729–5749.

Williams, J.E., Scheele, M.P., van Velthoven, P.F.J., Thouret, V., Saunois, M., et al., 2010. The influence of biomass burning on tropospheric composition over the tropical Atlantic Ocean and Equatorial Africa during the West African monsoon in 2006. Atmos. Chem. Phys. Discuss. 10, 7507–7552.